

Acoustic topology optimisation using CMA-ES

V. T. Ramamoorthy¹, E. Özcan¹, A. J. Parkes¹, A. Sreekumar², L. Jaouen³, F.X. Bécot³

¹ The University of Nottingham, School of Computer Science
Jubilee Campus, Nottingham NG8 1BB, United Kingdom

² The University of Nottingham, Faculty of Engineering, Centre for Structural Engineering and Informatics,
University Park Campus, Nottingham NG7 2RD, United Kingdom

³ Matelys Research Lab
No. 7 Rue des Maraîchers, Vaulx-en-Velin 69120, France

Abstract

Structural topology optimisation techniques are increasingly being applied to acoustic materials. Most acoustic topology optimisation applications use the solid-isotropic-material-with-penalization (SIMP) approach [1]–[4] which is a derivative-based method. In this work, we study the use of covariance-matrix-adaptation-evolution-strategy (CMA-ES) [5], [6], considered the state of the art approach for derivative-free continuous optimisation, as a candidate for acoustic topology optimisation. The performance of both CMA-ES and SIMP are compared on a small test problem. In this initial study, manufacturability restrictions and volume constraints were not considered for either of the algorithms. Comparisons show that SIMP quickly results in a good quality solution, while CMA-ES converges slowly but to a better quality solution.

1 Introduction

Composite materials are replacing conventional metals in automotive and aerospace applications due to their high strength-to-weight ratio. Since composites generally have poor acoustic isolation properties compared to metals [7], porous sound-absorbing materials are used alongside composites to keep the noise within acceptable limits. Researchers are interested in extracting the best performance from porous materials either by modifying their material parameters (such as porosity, static airflow resistivity, tortuosity etc) or their geometry (shape and topology). In this article, we focus on the shape and topology optimisation of porous materials.

Improving the shapes of sound-absorbing foams dates back to the 1940s when Beranek and Sleeper [8] conducted experiments on different shapes for sound-absorbing materials to use in anechoic chamber walls showing the promising performance of wedge shapes. Wedge shapes are still used in anechoic chambers to this day due to the simplicity in manufacturing. Using mathematical models instead of performing laboratory experiments to optimise foam shapes became possible only decades later, thanks to the development of modern finite element techniques, the development of accurate porous material models, and enhancement in computational capabilities. In the 1950s, Biot introduced a theory to model porous materials capturing the elastic effects of the solid part [9], [10]. In the 1970s, Zienkiewicz [11] pioneered the finite element method which is now widely researched and applied to model most engineering structures. Towards the end of the 20th century, researchers developed precise models to describe the visco-thermal dissipation in acoustical porous materials. Among these models, we will use the Johnson-Champoux-Allard-Lafarge (JCAL) [12]–[14]. A summary of the JCAL model and the Biot’s theory is presented in “Acoustical Porous Material Recipes” website [15]. As modern additive manufacturing techniques are becoming less expensive, intricate designs are becoming feasible to manufacture. Hence, finding the optimal shape or topology is of interest to the acoustic designers.

After the introduction of structural topology optimisation (STO) by Bendsøe and Kikuchi [1] in the late 1980s, many theoretical developments have taken place and a community of researchers are actively working in this area. Naturally, researchers could extend these techniques to acoustic design problems. STO has traditionally focused on the compliance minimisation problem [16] [17]. The application of topology optimisation to other problem domains has been steadily on the rise in the last two decades (2000-2020) ([18], [16], [19]). Within the acoustics domain, topology optimisation techniques have been successfully used on a variety of applications ranging from horns to mufflers ([20], [21] [22], [23], [24] [25] [26]). Although many approaches are available, Solid-Isotropic-Material-with-Penalty (SIMP) method is used as the optimisation technique in most of the applications: comparisons between different optimisation techniques are rare.

In this study, we present a comparison between the SIMP approach often called density-based topology optimisation, and the state of the art continuous optimisation algorithm CMA-ES (Covariance Matrix Adaptation Evolution Strategy). We obtain the trade-off solutions from SIMP-optimality criteria method by using various values for the volume fraction constraint, and from CMA-ES using a threshold filtering approach. The resulting solutions are compared. For the comparisons, we ignore the manufacturability restrictions and volume fraction constraints. The optimisation problem then becomes to find the optimal assignment of porous material or air in each of the elements in the design domain. To make the comparisons fair, we remove the filtering options in SIMP, since the purpose of filtering is solely to enforce manufacturable shapes while maintaining a minimum length scale. Such filtering techniques may be applied in the post-processing stage on the best solutions obtained from optimisation.

The outline of this article is as follows. We describe the mathematical model of a typical acoustic topology optimisation problem in section 2. In section 3, the details of the test problem instance used for comparing optimisation algorithms are given. The proposed CMA-ES based topology optimisation algorithm is described in section 4. The SIMP implementation is described in section 5. Subsequently, the results of the two algorithms are compared and deduced conclusions are described in sections 6 and 7, respectively.

2 Optimisation problem model

Acoustic Topology Optimisation (ATO) problem is to find the best distribution of air or porous materials in a design domain such that a desired acoustic parameter is optimised. Consider the finite element representation of an acoustic system, such as the one shown in Figure 1. The design domain is the collection of elements where each element is to be assigned either porous material properties or air properties. The goal of the problem is to find the optimal assignment $\chi_i \in \{0, 1\}$ to each element $i \in \{1, 2, \dots, N\}$ where $\chi_i = 0$ means the i^{th} element has properties of air and $\chi_i = 1$ means the i^{th} element has properties of a given porous material, such that a desired acoustic parameter (F) is optimised. This is expressed in equation 1. Here, N is the total number of elements in the design domain. The objective function (F) may be chosen based on the application, say, maximising the sound absorption coefficient or sound transmission loss, or minimizing sound pressure level at a point etc.

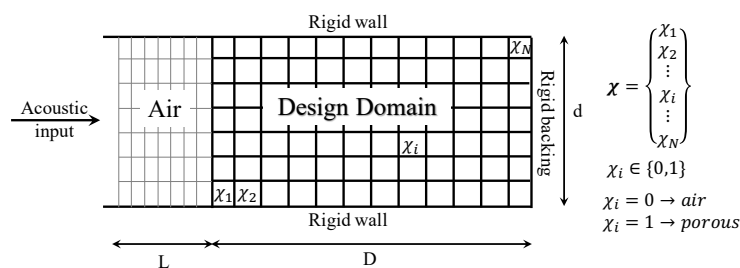


Figure 1: Problem representation in an acoustic topology optimisation problem instance.

$$\min_{\chi_i} F(\chi) \quad \text{where } F \in \mathbb{R}[0, 1], \quad \chi_i \in \{0, 1\} \quad (1)$$

The combinatorial problem could be relaxed to a continuous optimisation problem by considering $\chi_i \in (0, 1]$ instead of $\{0, 1\}$ to apply continuous optimisation techniques. The decision variables become design variables and the vector of design variables $\boldsymbol{\chi} = \{\chi_1, \chi_2, \dots, \chi_i, \dots, \chi_N\}^T$ describes a shape (a candidate solution). The SIMP interpolation scheme is used to assign intermediate material parameters for elements which are assigned χ_i between 0 and 1. All material parameters are interpolated using the power-law approach. In the power-law approach, a material parameter, say ψ , for the intermediate material is given by the equation 2.

$$\psi_i = \psi_{air} + \chi_i^p [\psi_{por} - \psi_{air}] \quad (2)$$

Here, ψ_{air} is the material parameter value of air, ψ_{por} is the value for the porous material considered, and ψ_i is the value assigned to i^{th} element. It satisfies the requirement that $\chi_i = 0 \rightarrow \psi = \psi_{air}$ and $\chi_i = 1 \rightarrow \psi = \psi_{por}$. Since the intermediate materials are non-existent, the material interpolation is penalised using the power law penalty p . For $\chi_i \in (0, 1)$ the element assigned the intermediate material is given a penalised effect, since $\chi_i^p < \chi_i$. This, combined with a volume fraction constraint $(1/N) \sum_i \chi_i \leq V_f$ is expected to implicitly push the optimised solutions towards $\chi_i = 0$ or 1. However, the power-law approach is not a hard condition and in several cases this does not impose $\chi_i \in \{0, 1\}$.

3 Test problem

For testing the optimisation approaches, a small test problem was chosen which is similar to the one considered in Lee *et al.* [22]. The difference in the present case is that instead of a rigid boundary on the sidewalls, a symmetric boundary is considered. A two-dimensional rectangular system with a height of 5.4 cm (d) backed by a rigid wall is considered as shown in Figure 1. The design domain is assumed from the rigid wall up to 13.5 cm (D). Followed by the design domain, a column of air with a thickness of 5.4 cm (L) is modelled using finite elements to compute the sound absorption coefficient. The porous material considered for the problem was assigned the parameters reported in Table 1. As unusual as these parameters may appear, they were used in Lee *et al.* [22] and they will only serve as an example here.

Table 1: Material parameters of the porous material used.

Property	Value	Units
Acoustic model	JCAL [12]–[14]	
Porosity (ϕ)	0.9	
Thermal characteristic length (Λ')	4.49e-04	(m)
Viscous characteristic length (Λ)	2.25e-04	(m)
Static airflow resistivity (σ)	25000	(N·s·m ⁻⁴)
High frequency limit of tortuosity (α_∞)	7.8	
Thermal permeability (k'_0)	4.75e-09	
Bulk density (ρ)	31.08	(kg·m ⁻³)
Young's modulus (E)	800000	(Pa)
Poisson's ratio (ν)	0.4	
Dissipation factor (η)	0.265	

The optimisation objective considered for the test problem is to maximise the average sound absorption coefficient (α) across a target frequency range. The target frequencies considered for the test problem are from 100 Hz to 1500 Hz in steps of 100 Hz. The acoustic input is given in the form of a normal incidence sound source at the left end. The alternative Biot's poroelastic finite element formulation for dissipative porous media [27] was used to model the system to compute the sound absorption coefficient. In this model, each node in the finite element mesh has three degrees of freedom, namely, the displacement of the solid frame in horizontal (U_x) and vertical directions (U_y), and the acoustic pressure of the fluid part (P). The visco-thermal properties of the porous material are described using the JCAL model [12]–[14]. The boundary conditions and the loads are applied and the resulting displacement and pressure fields (U_x , U_y and P) are

obtained at each frequency by solving the finite element problem. From these fields, the sound absorption is computed by using the impedance method. Then the optimisation problem is as described by equation 3 i.e. to find the best assignment $\boldsymbol{\chi}^* = \{\chi_1^*, \chi_2^*, \dots, \chi_i^*, \dots, \chi_N^*\}^T$ such that the sound absorption coefficient averaged over the target frequencies ($\bar{\alpha}$) is maximised: the objective function $F = 1 - \bar{\alpha}$ is to be minimised.

$$\min_{\boldsymbol{\chi}_i} F(\boldsymbol{\chi}) = 1 - \bar{\alpha} \quad (3)$$

$$\text{where } \bar{\alpha} = \frac{1}{n} \sum_{f=f_1}^{f_n} \alpha(\boldsymbol{\chi}, f), \quad \bar{\alpha} \in \mathbb{R}[0, 1], \quad \chi_i \in \{0, 1\} \quad (4)$$

4 Covariance Matrix Adaptation Evolution Strategy (CMA-ES)

Covariance Matrix Adaptation - Evolution Strategy is a state of the art black-box optimisation algorithm for continuous optimisation which has outperformed most other evolutionary algorithms in hundreds of applications [28] (black-box means that it only uses the result of the fitness evaluation, and does not use the internal structure of the fitness, in particular, does not use derivatives). CMA-ES constructs a multivariate Gaussian response surface by iteratively sampling points in the search space and adapting the covariance matrix of the multivariate Gaussian to perform the search. The MATLAB implementation for CMA-ES provided by Hansen [6] is adopted for performing topology optimisation. The full algorithm and procedure are not discussed in this article as it can be found in numerous others. The pseudocode for topology optimisation using CMA-ES is provided in algorithm 1.

In this application, the unconstrained CMA-ES was modified to include upper and lower limit constraints on the design variables. To ensure χ_i is not below 0 or above 1, after the CMA-ES samples points within the N dimensional hypercube ($\chi_i \in [0, 1] \quad \forall \quad i \in 1 \dots N$), the values below 0 were forced to be equal to 0 and the values above 1 were forced to be equal to 1.

In the implementation, strategy parameters for selection, adaptation, dynamic strategy parameters and constants were as in the MATLAB code by Hansen [6]. The lines 24-28 in the pseudocode 1 are elaborated in the paper by Hansen [6]. In the pseudocode, $I_{N \times N}$ is the identity matrix of size $N \times N$. λ is the population size. The expression $\text{randn}(N, 1)$ generates a vector of random numbers of size N from the standard normal distribution. The function $\text{diag}()$ returns the elements in the leading diagonal of a square matrix. A nominal maximum number of function evaluations (budget) of 4096 was set as the termination criterion.

Since CMA-ES is not a deterministic algorithm (based on random numbers; reruns may not produce the same results), the performance cannot be ascertained with one trial run. Hence, to produce statistically meaningful performance tests, 31 trials of CMA-ES were run with different random number seeds, each with a budget of 4096 finite element function evaluations.

The CMA-ES solutions did not result in 0 or 1 shapes in most trials despite using the recommended value for the material interpolation penalty ($p = 3$). Many elements had χ_i between 0 and 1 which correspond to intermediate materials between air and the porous material. Since intermediate materials are not physically realistic, a simple round-off filter was used for the final best solutions to get 0 or 1 solutions $\bar{\boldsymbol{\chi}}^* = \lfloor \boldsymbol{\chi}^* \rfloor$. The rounding filter is expressed in equation 5. An illustration of rounding the best shape from one of the trials is provided in Figure 2.

$$\bar{\boldsymbol{\chi}}^* = \text{round}(\boldsymbol{\chi}^*) = \lfloor \boldsymbol{\chi}^* \rfloor = \{\lfloor \chi_1^* \rfloor, \lfloor \chi_2^* \rfloor, \dots, \lfloor \chi_i^* \rfloor, \dots, \lfloor \chi_N^* \rfloor\}^T \quad (5)$$

$$\lfloor x \rfloor = \begin{cases} 0 & \text{when } 0 < x \leq 0.5 \\ 1 & \text{when } 0.5 < x \leq 1 \end{cases} \quad (6)$$

Algorithm 1: An application of CMA-ES to acoustic topology optimisation

```

1 Get finite element mesh, frequencies, material properties and other common parameters;
2 Initiate  $\chi_{mean} \leftarrow \text{rand}(N,1)$ ,  $\sigma \leftarrow 3$  and  $B \leftarrow I_{N \times N}$ ;
3 Set population size,  $\lambda \leftarrow 4 + \lfloor 3 \log(N) \rfloor$ ;
4 Set strategy parameters for selection;
5 Set strategy parameters for Adaptation;
6 Initialize dynamic strategy parameters and constants;
7 Set  $fevals \leftarrow 0$ ;
8 while  $fevals < budget$  do
9   for  $k = 1, k \leq \lambda, i++$  do
10     $\chi^{(k)} \leftarrow \chi_{mean} + \sigma[B]D \times \text{randn}(N,1)$ ; // sampling candidate solutions
11    for  $i = 1, i \leq N, i++$  do
12      if  $\chi_i^{(k)} < 0$  then
13         $\chi_i^{(k)} = 0$ ; // If element interpolation parameter <0, set it to 0
14      end
15      if  $\chi_i^{(k)} > 1$  then
16         $\chi_i^{(k)} = 1$ ; // If element interpolation parameter >1, set it to 1
17      end
18    end
19    Assemble FE system matrices;
20    Evaluate absorption  $\alpha(\chi^{(k)})$ ; // solve FE problem
21    Set  $fevals \leftarrow fevals + 1$ ;
22    Set  $F(\chi^{(k)}) = 1 - \alpha(\chi^{(k)})$ ; // setting  $(1-\alpha)$  as the objective  $F$  to be minimised
23  end
24  Sort by fitness and compute weighted mean into  $\chi_{mean}$ ;
25  Cumulation: Update evolution paths;
26  Adapt covariance matrix  $[C]$ ;
27  Adapt step size  $\sigma$ ;
28  Decomposition of  $[C]$  into  $[B]\text{diag}([D]^2)[B]'$ ; // diagonalisation
29  Update best shape  $\chi^* \leftarrow \text{best}(\chi^*, \chi^{(k)})$ 
30 end
31 return Best  $\chi^*$ ;
    
```

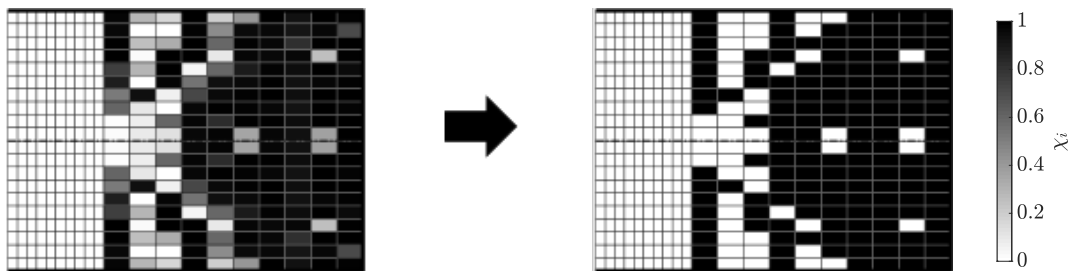


Figure 2: An illustration of rounding best shape from trial 14 of CMA-ES to get 0 or 1 shapes. The colors corresponding to the values 0 and 1 indicates air and porous material respectively.

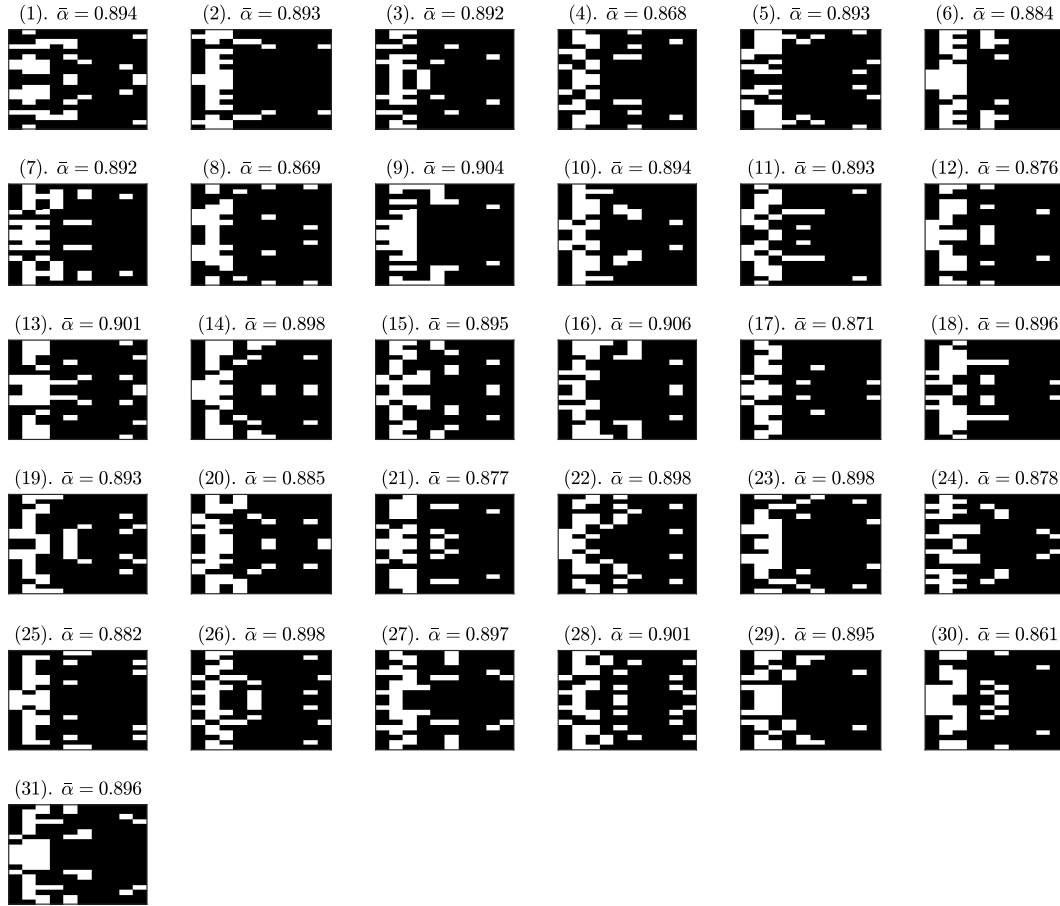


Figure 3: Rounded best solutions from all 31 trial runs of CMA-ES with trial number in parenthesis and the recomputed mean sound absorption $\bar{\alpha}$.

The best results from all the trials are rounded to 0 or 1 solutions using the equation 5. The rounded best shapes and their corresponding mean sound absorption frequencies across the target frequency range are plotted in Figure 3. Rounding off results in a small reduction in absorption values for both CMA-ES and SIMP solutions as expected. Hence, the comparison will be made only with rounded solutions from both CMA-ES and SIMP.

5 Solid Isotropic Material with Penalization (SIMP)

Solid Isotropic Material with Penalization (SIMP) scheme is a derivative-based continuous optimisation approach to optimise the distribution of materials in a finite element mesh so as to minimise or maximise a structural parameter. Topology optimisation using homogenization was first introduced by Bendsøe and Kikuchi [1] and the SIMP method was later developed [2], [3], [17]. An array of methods are now available for topology optimisation as discussed in [17] including the level-set and phase-field methods, however, SIMP remains the most popular method of choice for topology optimisation and is considered the state of the art. The algorithm is simple that it can be implemented in less than 100 lines of code as shown by Sigmund [4]. Later, even a more efficient version was published by Andreassen *et al.* [29].

SIMP based topology optimisation is widely applied to the compliance minimisation problem (equation 7).

$$\min_{\chi} \quad c(\chi) \quad \text{subject to:} \quad \frac{1}{N} \sum_i \chi_i \leq V_f \quad (7)$$

Here $c \in \mathbb{R}$ is the compliance of the structure to be minimised, subject to a volume fraction constraint V_f .

SIMP has been applied on acoustic topology optimisation in numerous occasions [21]–[24]. As mentioned previously, for the test problem the volume fraction constraint is not considered and no manufacturability filtering is used for fair comparison with CMA-ES.

Algorithm 2: An application of the SIMP approach to acoustic topology optimisation

```

1 Get finite element mesh, frequencies, material properties and other common parameters;
2 Initiate  $\chi_{init} \leftarrow V_f \times \text{ones}(N,1)$ ;
3 Set  $\chi \leftarrow \chi_{init}$ ;
4 while Termination criteria is NOT met do
5     Assemble the FE global matrices using  $\chi$  and calculated material properties at each frequency;
6     Evaluate absorption coefficients at each frequency  $\alpha(\chi, f)$ ;
7     Evaluate derivatives at each frequency  $(d\alpha/d\chi)_f$ ;
8     Set  $c = 1 - \sum_f \alpha(\chi, f)$ ; // c to be minimised
9     Set the sensitivities  $dc/d\chi = -\sum_f (d\alpha/d\chi)_f$ ;
10    Skip filtering;
11    Update of design variables  $\chi_{new} \leftarrow \text{OptiCriteria}(\chi, c, dc/d\chi)$ ;
12    Set  $\chi = \chi_{new}$ ;
13 end
14 return Best  $\chi^* \leftarrow \chi$ ;
    
```

A maximum of 200 finite element function evaluations is allowed as the termination criterion. The objective in the test problem is to maximise absorption irrespective of the volume fraction, however, when a specific volume fraction constraint is set in SIMP, the algorithm finds solutions near that volume fraction. Hence six trials of SIMP are run with different volume fraction constraints, picked from $\{0.25, 0.5, 0.6, 0.7, 0.8, 1.0\}$ and the best is used for comparison. The best results before and after rounding off are given in Figure 4. As can be seen from the figure, for this problem instance, the best result before rounding is obtained from a trial with volume fraction constraint 1.0, whereas after rounding the trial with volume fraction constraint 0.5 turned out to be the best.

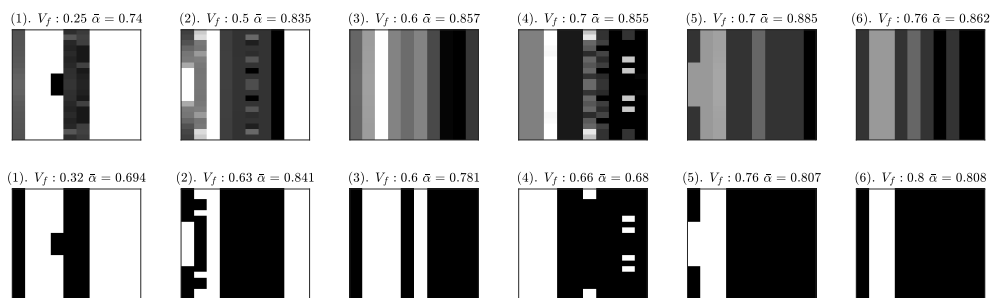


Figure 4: Best shapes from SIMP method with volume fraction constraints (1). $V_f = 0.25$ (2). $V_f = 0.5$ (3). $V_f = 0.6$ (4). $V_f = 0.7$ (5). $V_f = 0.8$ (6). $V_f = 1.0$. The solutions found by SIMP may have different volume fractions from the one specified. The actual volume fractions of the found solutions are displayed above each best shape. The rounded shape from each of these trials is printed below the corresponding raw shape from each trial.

6 Results

Absorption achieved vs Computational time

To reduce the computational time, only the lower half of the 2-dimensional system is modelled using and a symmetric boundary condition was used on the line of symmetry. The absorption values computed from the lower half finite element model with a symmetric boundary condition were verified with those from the full

model assuming symmetrically placed elements. Further, the use of sparse matrices for assembly and solving significantly improved the computational speed. Since CMA-ES is a derivative-free algorithm, each function evaluation takes significantly less time. For SIMP, the derivative computation time is reduced considerably by computing the inverse of the system matrix explicitly and using it to evaluate the derivatives. The average times per finite element evaluation with and without derivatives are computed on the same machine (see Table 2). To compare the performance of CMA-ES and SIMP, the progress of mean absorption with computational time is plotted in Figure 5. For SIMP, only the trial with volume fraction 1.0 which produces the highest absorption among the SIMP trials is considered. Since CMA-ES is not a deterministic algorithm, the results differ from trial to trial. Hence, for CMA-ES the absorptions ($\bar{\alpha}$) from all 31 trials were averaged at each function evaluation (feval) step. It can be seen that the SIMP algorithm converges after a few hundred seconds to a good absorption value. Whereas CMA-ES is relatively slow but finds solutions with better absorption.

Table 2: Average time per finite element function evaluation (feval)

Algorithm	Optimisation type	Requested O/Ps	Budget	Total time	Avg time per feval
CMA-ES	derivative-free	$\alpha(\chi)$	4096	2508 s	0.6123 s
SIMP	derivative-based	$\alpha(\chi)$ and $d\alpha/d\chi_i$	200	3148 s	15.74 s

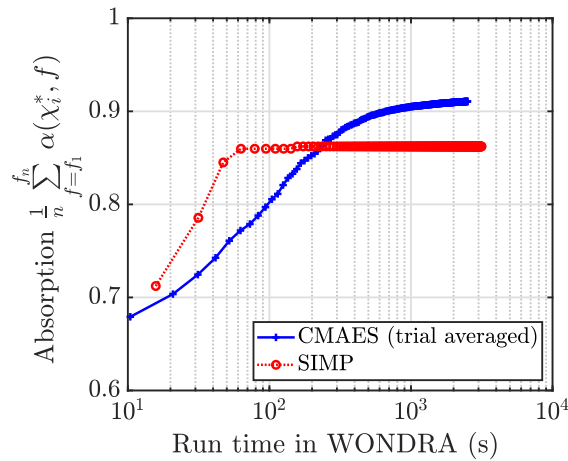


Figure 5: Best fitness progress compared between (1) CMA-ES (averaged over 31 trials) and (2) SIMP optimality criteria method with no filtering (best trial with volume fraction constraint $V_f = 1.0$).

Distribution of mean sound absorption of best solutions from all trial runs

Since the raw best solutions from both CMA-ES and SIMP had intermediate materials (χ_i between 0 and 1), a rounding-off filter was used to discretise the final results to get 0 or 1 solutions. The discretising final solutions were solved using the finite element solver to recompute the absorption values. A comparison of the distribution of the raw final mean absorption values and the mean absorption values of the rounded final solutions is shown in Figure 6. For SIMP, the distribution of mean absorption values of the raw best solutions computed from 6 trials with different volume fractions is also shown, along with the distribution of mean absorption values of rounded best solutions. It is observed that after discretisation, the quality of the solutions (mean absorption) reduce slightly for both CMA-ES and SIMP results.

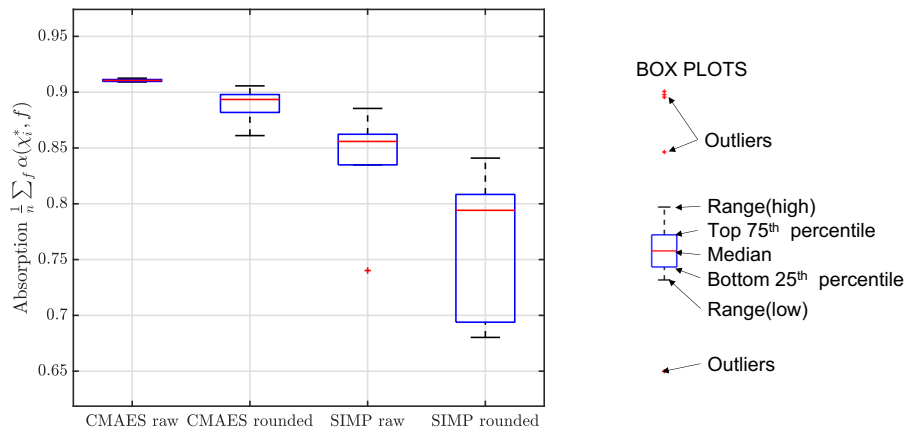


Figure 6: Best fitness distribution compared between (1) CMA-ES (averaged over 31 trials) allowing upto 4096 finite element evaluations (2) SIMP optimality criteria method with no filtering upto 200 finite element evaluations. The schematic on the right gives the labels for the box plots.

Comparison of absorption curves of the best shapes from the CMA-ES and SIMP

The discretised best shapes from one of the trials of CMA-ES and the SIMP trial with volume fraction constraint 0.5 are picked for comparison. The absorption curves for these shapes are plotted in Figure 7. During optimisation, frequencies considered are only in steps of 100 Hz to reduce optimisation time.

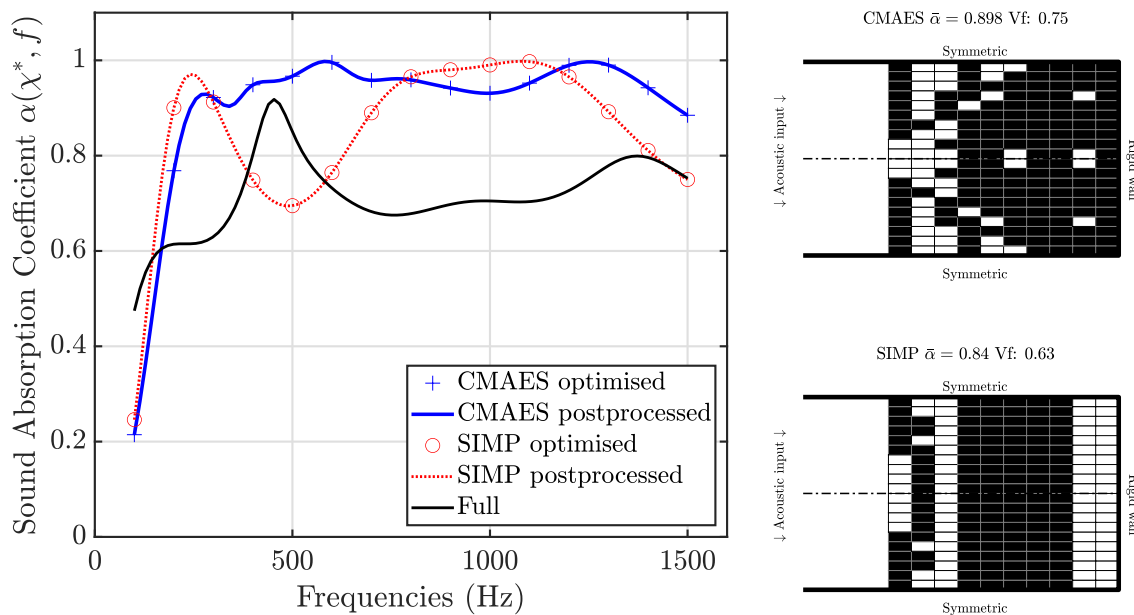


Figure 7: Best shapes evaluated from CMA-ES and SIMP, and their absorption curves. The CMA-ES solution is picked from trial run 14 and the SIMP solution is picked from the run with volume fraction constraint $V_f = 0.5$. The absorption curves were recomputed for more frequencies in post-processing. On the right, the corresponding best shapes from CMA-ES and SIMP are shown. Full indicates the absorption curve for fully filled design domain.

Threshold filtering study

To obtain solutions with the desired volume fraction V_f from a CMA-ES trial, a threshold filtering approach may be used. This has also been suggested in [17]. To do this, the elements in the design domain are sorted

according to the values of design variables in the final solution obtained from a CMA-ES trial χ_i^* . The highest ($V_f \times N$) number of elements which have the highest χ_i values are set to 1 and the rest are set to 0. This is a simple way to enforce volume fraction constraint on CMA-ES solutions. Applying such an approach on the best shape from trial 14 of CMA-ES for volume fractions in steps of 0.1 resulted in shapes which had porous elements suspended in air (see Figure 8) for low volume fractions. Notably, threshold filtering may be inferior compared to rounding, since the latter preserves to some degree the physical presence or absence of material as that of the optimised shape. There are several articles describing filtering techniques in topology optimisation [30], [31], [32]. These filtering techniques may be used during the optimisation or in post-processing for finding manufacturable solutions. The objective function can be recomputed after filtering the solutions to ensure that the quality (fitness) is preserved prior to finalizing the designs for manufacturing. This was one reason to not consider manufacturability in this study. The other reason to ignore manufacturability restrictions is the interest of finding solutions closer to the true optimum without bias.

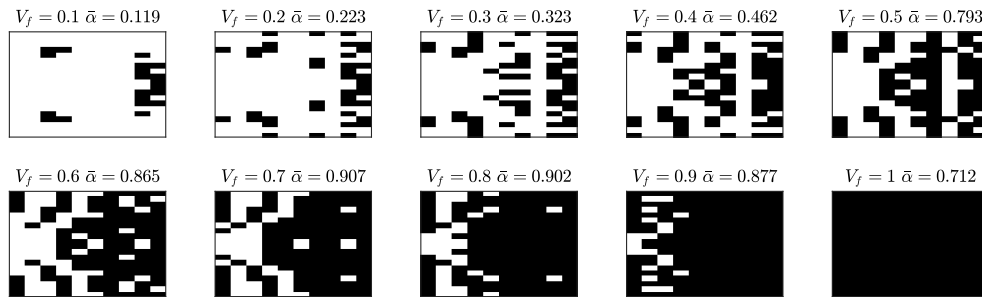


Figure 8: Threshold filtering of CMA-ES solutions with various volume fraction constraints ranging from 0.1 up to 1.0 in steps of 0.1

Summary

Overall, both CMA-ES and SIMP resulted in solutions with some element densities (χ_i) between 0 and 1, and hence the best solutions were rounded for comparison. The best solutions from all CMA-ES trials were higher in absorption than SIMP solutions both before and after rounding-off, for this problem instance and for the budget considered. This is likely due to the fact that the landscape is either multi-modal or noisy resulting in SIMP reaching a local optimum prematurely. Since, CMA-ES is a global optimisation approach known for performing well on ill-conditioned and noisy landscapes, by carefully sampling points and constructing the multivariate Gaussian response surface, better quality solutions are reached. However, if only a lower run time budget had been allowed, SIMP would have outperformed CMA-ES. This indicates that none of the two algorithms compared can be considered to outperform the other in all aspects and a trade-off needs to be made.

For large problem instances (large N), CMA-ES may take a large number of function evaluations before a better solution than that of SIMP is reached. The drawback of using derivative-free approaches is that they are not mesh-independent i.e. large N problems could take a large amount of time. However, for some problem domains with noisy landscapes, the solutions obtained from derivative-based approaches like SIMP might not be close to the true optimum. In addition to this, in very large N problems, the derivative computation can be too expensive. Thus, there exists a large scope for developing new and improved optimisation approaches that are both fast and efficient (find solutions closer to the true optimum).

7 Conclusion

In this work, topology optimisation for acoustic sound-absorbing materials was performed using a covariance matrix adaptation evolution strategy (CMA-ES). The performance of CMA-ES was compared with that of Solid-Isotropic-Material-with-Penalisation scheme (SIMP), for a test problem in the acoustic domain with no manufacturability restrictions and no volume fraction constraint. The objective was to simply maximise

the absorption by assigning the best choice between air and porous material for each element in the design domain. The trivial fully-porous design is not the optimum solution for this problem instance. Thirty-one trials of CMA-ES with different random number seeds and six trials of SIMP with different volume fraction constraints were run on the test problem. A budget of 4096 derivative-free finite element evaluations was allowed for CMA-ES and a budget of 200 derivative-included finite element evaluations was allowed for SIMP which take about the same run time. Rounding was done to ensure 0-1 solutions are produced. The best solution from SIMP was a flat-layered shape whereas CMA-ES gives a wedge-like shape. The best solutions from all CMA-ES trials were better than SIMP solutions both before and after rounding-off, for this problem instance and for the runtime budget considered. SIMP converged quickly to better quality solutions initially. If a lower runtime budget had to be considered, SIMP would outperform CMAES on this problem instance. Neither algorithm can be considered to be superior to the other in all aspects. If a good solution is needed quickly, SIMP seems to be the right choice and if a better quality solution is needed, CMA-ES might be preferable.

Acknowledgement

This result is part of a project that has received funding from the European Research Council (ERC) under the European Union's Horizon 2020 research and innovation programme *No2Noise* (no2noise.eu) with grant agreement No. 765472).

References

- [1] M. P. Bendsoe and N. Kikuchi, "Generating optimal topologies in structural design using a homogenization method," 1988.
- [2] M. P. Bendsøe, "Optimal shape design as a material distribution problem," *Structural optimization*, vol. 1, no. 4, pp. 193–202, 1989.
- [3] M. Zhou and G. Rozvany, "The coc algorithm, part ii: Topological, geometrical and generalized shape optimization," *Computer methods in applied mechanics and engineering*, vol. 89, no. 1-3, pp. 309–336, 1991.
- [4] O. Sigmund, "A 99 line topology optimization code written in matlab," *Structural and multidisciplinary optimization*, vol. 21, no. 2, pp. 120–127, 2001.
- [5] N. Hansen and A. Ostermeier, "Completely derandomized self-adaptation in evolution strategies," *Evolutionary computation*, vol. 9, no. 2, pp. 159–195, 2001.
- [6] N. Hansen, "The cma evolution strategy: A tutorial," *arXiv preprint arXiv:1604.00772*, 2016.
- [7] D. Chronopoulos, M. Ichchou, B. Troclet, and O. Bareille, "Predicting the broadband response of a layered cone-cylinder-cone shell," *Composite Structures*, vol. 107, pp. 149–159, 2014.
- [8] L. L. Beranek and H. P. Sleeper Jr, "The design and construction of anechoic sound chambers," *The Journal of the Acoustical Society of America*, vol. 18, no. 1, pp. 140–150, 1946.
- [9] M. A. Biot, "Theory of elastic waves in a fluid-saturated porous solid. 1. low frequency range," *The Journal of the acoustical Society of america*, vol. 28, no. 1, pp. 168–178, 1956.
- [10] M. A. Biot, "Theory of propagation of elastic waves in a fluid-saturated porous solid. ii. higher frequency range," *The Journal of the acoustical Society of america*, vol. 28, no. 2, pp. 179–191, 1956.
- [11] O. C. Zienkiewicz, R. L. Taylor, P. Nithiarasu, and J. Zhu, *The finite element method*. McGraw-hill London, 1977, vol. 3.
- [12] D. L. Johnson, J. Koplik, and R. Dashen, "Theory of dynamic permeability and tortuosity in fluid-saturated porous media," *Journal of fluid mechanics*, vol. 176, pp. 379–402, 1987.
- [13] Y. Champoux and J.-F. Allard, "Dynamic tortuosity and bulk modulus in air-saturated porous media," *Journal of applied physics*, vol. 70, no. 4, pp. 1975–1979, 1991.

- [14] D. Lafarge, P. Lemarinier, J. F. Allard, and V. Tarnow, "Dynamic compressibility of air in porous structures at audible frequencies," *The Journal of the Acoustical Society of America*, vol. 102, no. 4, pp. 1995–2006, 1997.
- [15] L. Jaouen, "Acoustical porous material recipes," *Website URL: <http://apmr.matelys.com>, ISSN 2606-4138*, 2000-2020.
- [16] M. P. Bendsoe and O. Sigmund, *Topology optimization: theory, methods, and applications*. Springer Science & Business Media, 2013.
- [17] O. Sigmund and K. Maute, "Topology optimization approaches," *Structural and Multidisciplinary Optimization*, vol. 48, no. 6, pp. 1031–1055, 2013.
- [18] G. Rozvany, "Aims, scope, methods, history and unified terminology of computer-aided topology optimization in structural mechanics," *Structural and Multidisciplinary Optimization*, vol. 21, no. 2, pp. 90–108, 2001.
- [19] J. D. Deaton and R. V. Grandhi, "A survey of structural and multidisciplinary continuum topology optimization: Post 2000," *Structural and Multidisciplinary Optimization*, vol. 49, no. 1, pp. 1–38, 2014.
- [20] E. Wadbro and M. Berggren, "Topology optimization of an acoustic horn," *Computer methods in applied mechanics and engineering*, vol. 196, no. 1-3, pp. 420–436, 2006.
- [21] M. B. Dühring, J. S. Jensen, and O. Sigmund, "Acoustic design by topology optimization," *Journal of sound and vibration*, vol. 317, no. 3-5, pp. 557–575, 2008.
- [22] J. S. Lee, Y. Y. Kim, J. S. Kim, and Y. J. Kang, "Two-dimensional poroelastic acoustical foam shape design for absorption coefficient maximization by topology optimization method," *The Journal of the Acoustical Society of America*, vol. 123, no. 4, pp. 2094–2106, 2008.
- [23] G. H. Yoon, "Acoustic topology optimization of fibrous material with delany–bazley empirical material formulation," *Journal of Sound and Vibration*, vol. 332, no. 5, pp. 1172–1187, 2013.
- [24] W. U. Yoon, J. H. Park, J. S. Lee, and Y. Y. Kim, "Topology optimization design for total sound absorption in porous media," *Computer Methods in Applied Mechanics and Engineering*, vol. 360, p. 112 723, 2020.
- [25] Y. Xu, W. Zhao, L. Chen, and H. Chen, "Distribution optimization for acoustic design of porous layer by the boundary element method," *Acoustics Australia*, pp. 1–13, 2020.
- [26] L. Chen, C. Lu, H. Lian, Z. Liu, W. Zhao, S. Li, H. Chen, and S. P. Bordas, "Acoustic topology optimization of sound absorbing materials directly from subdivision surfaces with isogeometric boundary element methods," *Computer Methods in Applied Mechanics and Engineering*, vol. 362, p. 112 806, 2020.
- [27] F.-X. Bécot and L. Jaouen, "An alternative biot's formulation for dissipative porous media with skeleton deformation," *The Journal of the Acoustical Society of America*, vol. 134, no. 6, pp. 4801–4807, 2013.
- [28] N. Hansen, *References to cma-es applications*, 2005.
- [29] E. Andreassen, A. Clausen, M. Schevenels, B. S. Lazarov, and O. Sigmund, "Efficient topology optimization in matlab using 88 lines of code," *Structural and Multidisciplinary Optimization*, vol. 43, no. 1, pp. 1–16, 2011.
- [30] B. Bourdin, "Filters in topology optimization," *International journal for numerical methods in engineering*, vol. 50, no. 9, pp. 2143–2158, 2001.
- [31] O. Sigmund, "Morphology-based black and white filters for topology optimization," *Structural and Multidisciplinary Optimization*, vol. 33, no. 4-5, pp. 401–424, 2007.
- [32] B. S. Lazarov and O. Sigmund, "Filters in topology optimization based on helmholtz-type differential equations," *International Journal for Numerical Methods in Engineering*, vol. 86, no. 6, pp. 765–781, 2011.